DOI: 10.1002/ejic.200500568

Syntheses, Crystal Structures and Magnetic Properties of Carboxylato-Bridged Polymeric Networks of Mn^{II}

Subal Chandra Manna,[a] Ennio Zangrando,[b] Michael G. B. Drew,[c] Joan Ribas,*[d] and Nirmalendu Ray Chaudhuri*[a]

Keywords: Manganese(II) / Carboxylate / Crystal structure / Magnetic behavior

Three new carboxylato-bridged polymeric networks of Mn^{II} having molecular formula $[Mn(ox)(dpyo)]_n$ (**1**), $\{[Mn_2(mal)_2(bpee)(H_2O)_2]\cdot 0.5(bpee)\cdot 0.5(CH_3OH)\}_n$ (**2**) and $\{[Mn_3(btc)_2(2,2'\text{-bipy})_2(H_2O)_6]\cdot 4H_2O\}_n$ (**3**) [dpyo, 4,4′-bipyridine *N*,*N*′-dioxide; bpee, *trans*-1,2 bis(4-pyridyl)ethylene; 2,2′-bipy, 2,2′-bipyridine; ox = oxalate dianion; mal = malonate dianion; btc = 1,3,5-benzenetricarboxylate trianion] have been synthesized and characterized by single-crystal X-ray diffraction studies and low temperature magnetic measurements. Structure determination of complex **1** reveals a covalent bonded 2D network containing bischelating oxalate and bridging dpyo; complex **2** is a covalent bonded 3D polymeric architecture, formed by bridging malonate and bpee ligands, resulting in an open framework with channels filled by uncoordinated disordered bpee and methanol molecules. Whereas complex **3**, comprising btc anions bound to three metal centers, is a 1D chain which further extends its dimensionality to 3D via π-π and H-bonding interactions. Low temperature magnetic measurements reveal the existence of weak antiferromagnetic interaction in all these complexes.

Introduction

Metal-organic frameworks (MOFs) containing paramagnetic metal ions represent a new class of materials for their intriguing network topologies and for their potential applications in the area of catalysis, separation, sorption, sensors, but also as electronic and magnetic devices.[1,2] Moreover, such MOFs have compositional/structural diversities which may be tuned by the suitable choice of ligands as well as metal ions. Thus, the construction of target molecules with the properties mentioned above is a challenge for synthetic chemists.[3] To achieve the desired networks, various carboxylates have been used due to their wide variety of coordination modes,[4] resulting in efficient superexchange pathways. Several groups as well as our labs[5–8] reported the syntheses and characterizations of a large number of carboxylato-bridged multidimensional networks. Oxalate, malonate, succinate, fumarate, maleate, terephthalate, 1,3,5-benzenetricarboxylate etc. are among the more employed carboxylates to build up the framework. Moreover, combination of nitrogen donor co-/bridging- ligands i.e. pyrazine, piperazine, 1,2-bis(4-pyridyl)ethane, 4,4′-trimethylenedipyridine, 4,4′-bipyridyl disulphide, hexamethylenetetramine etc. with carboxylates may enhance the dimensionality of the molecular frameworks.[7] But evaluation of magnetic interaction of these coordination polymers as a function of geometry and electronic configuration of the individual metal ion is the most important issue in the current research.[9,10] Manganese-carboxylates are well recognized from the magnetic point of view[11,12] as these systems often possess a large number of unpaired electrons. Literature survey reveals[13] that there are several manganese-containing networks showing single molecular magnetism, ability of individual molecules to function as magnetizable magnets in the absence of an external magnetic field and with no long-range ordering from intermolecular interactions. Due to these novel properties, increasing attention has been devoted to the construction of manganese–carboxylate frameworks in order to assess the correlation between structure and magnetism.

While manganese–oxalate frameworks are rare,[14] there are some reports[15] on the molecular-based magnets formed by bimetallic three-dimensional oxalate networks. On the other hand, there are some reports by our group using malonate,[6] showing antiferromagnetic coupling only, besides interesting networks. Our studies till date did not investigate the effect of coligand on the magnetic property in the manganese-malonate frameworks. In addition, metal carboxylates, alone and in combination with nitrogen donor

[a] Department of Inorganic Chemistry, Indian Association for the Cultivation of Science,
Kolkata 700032, India
Fax: +91-33-2473-2805
E-mail: icnrc@iacs.res.in
[b] Dipartimento di Scienze Chimiche, University of Trieste, 34127 Trieste, Italy
[c] Department of Chemistry, The University of Reading, Whiteknights, Reading RG6 6AD, UK
[d] Departament de Química Inorgànica. Universitat de Barcelona, Diagonal, 647, 08028 Barcelona, Spain
E-mail: joan.ribas@qi.ub.es
Supporting information for this article is available on the WWW under http://www.eurjic.org or from the author.

coligands, are of particular interest for the possibility to form open-framework structures[4b] besides the existence of magnetic interactions. The above mentioned facts have driven us to pursue the design and syntheses of manganese–carboxylates varying the carboxylate anion as well as the coligand.

The present contribution reports the syntheses, crystal structures and low-temperature magnetic measurements of three new carboxylato-bridged polymeric architectures of manganese(II) using three different carboxylates, $[Mn(ox)(dpyo)]_n$ (**1**), $\{[Mn_2(mal)_2(bpee)(H_2O)_2]\cdot 0.5(bpee)\cdot 0.5(CH_3OH)\}_n$ (**2**) and $\{[Mn_3(btc)_2(2,2'\text{-bipy})_2(H_2O)_6]\cdot 4H_2O\}_n$(**3**) [dpyo = 4,4′-bipyridine *N*,*N*′-dioxide; bpee = *trans*-1,2-bis(4-pyridyl)ethylene; 2,2′-bipy = 2,2′-bipyridine; ox = oxalate dianion; mal = malonate dianion; btc = 1,3,5-benzenetricarboxylate trianion].

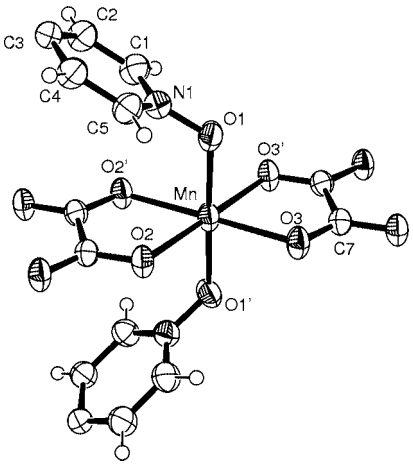

Figure 2. ORTEP drawing of the manganese coordination sphere in complex **1**. The metal is located on a twofold axis passing in between the oxalate C–C bond.

Results and Discussion

Description of the Structures

Complex 1

The X-ray diffraction analysis of complex **1** displays a 2D layered structure of composition $[Mn(ox)(dpyo)]_n$, as depicted in Figure 1. In the framework of (4,4) topology, the manganese ions occupy the 4-connecting nodes while double chelating oxalate and dpyo ligands form the rhomboid grid, with the latter spacers arranged in a herringbone pattern with respect to the –Mn–ox– arrays. The metals are separated by 5.657(2) Å (axis b) along the oxalate and by 12.537(3) Å through the dpyo linkers. Each manganese(II) center is arranged on a twofold axis and the coordination sphere comprises of *trans*-located dpyo oxygen atoms and four oxalate donors in the equatorial plane (Figure 2). All the Mn–O bond lengths are comparable in length within their e.s.d.'s. (Table 1). The dpyo ligand, positioned on a center of symmetry, presents coplanar pyridine rings and is connected to the metal with a N(1)–O(1)–Mn angle of 119.8(2)°.

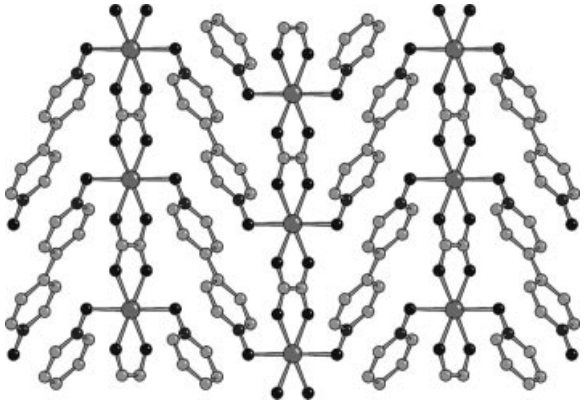

Figure 1. Ball and stick drawing of the 2D sheet of complex **1**.

Table 1. Selected coordination bond lengths [Å] and angles [°] of complex **1**.

Mn–O(3)	2.175(2)	Mn–O(2)	2.185(2)
Mn–O(1)	2.180(2)	O(1)–N(1)	1.332(4)
O(2)–Mn–O(2′)	75.64(11)	O(3)–Mn–O(1)	87.63(9)
O(3′)–Mn–O(3)	77.40(12)	O(3)–Mn–O(2)	103.48(8)
O(1)–Mn–O(1′)	178.60(14)	O(3)–Mn–O(2′)	179.12(9)
O(1)–Mn–O(2)	88.81(9)	C(7)–O(2)–Mn	115.70(19)
O(1′)–Mn–O(2)	92.30(9)	C(7′)–O(3)–Mn	113.49(19)
O(3′)–Mn–O(1)	91.28(9)	N(1)–O(1)–Mn	119.8(2)

The packing shows well-separated layers and the shortest intermetallic distance is 7.648(2) Å. The shortest contact of 3.315(4) is detected between C(1) and O(2) that can be interpreted as a CH···O interaction.

Complex 2

The structure of **2** reveals covalently bonded $[Mn(mal)(H_2O)]_n$ layers connected by bpee ligands to form a 3D polymer (Figure 3 and Figure 4). The malonate anion, in its frequently found coordination mode[6,16,17] acts as a chelating and a bis(monodentate) ligand towards three metal ions. A selection of bond lengths and angles is reported in Table 2, and the metal coordination sphere with atom labeling Scheme is shown in Figure 5. The octahedral coordination geometry of the metal atom consists of four planar equatorial carboxylate oxygen atoms [range of Mn–O bond lengths of 2.165(3)–2.183(3) Å], while the axial positions are occupied by a water molecule and a bpee nitrogen donor with slightly longer bond lengths [Mn–O(1w) 2.263(3), Mn–N(21) 2.297(3) Å, Table 2].

In the (4,4) square grid (Figure 3) of side dimensions 5.419 × 5.614 Å (Mn–Mn distances), the coordinated water molecule forms two intra-layer hydrogen bonds with oxygen atoms of the neighboring chelating anions [O(1w)–O(17) 2.719(5) Å, O(1w)–O(11) 2.748(4) Å].

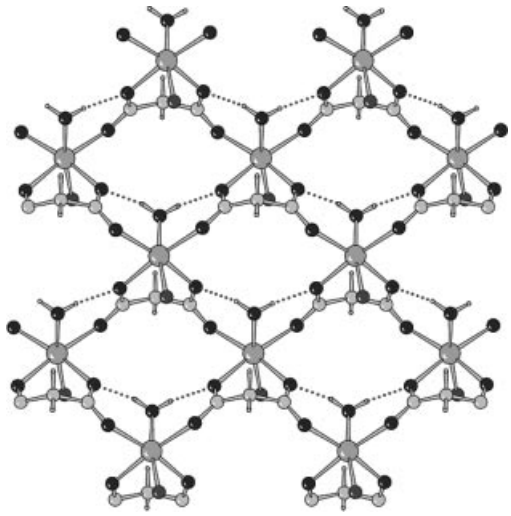

Figure 3. Corrugated $[Mn(H_2O)(mal)]_n$ layers in complex **2** down axis *b* (only nitrogen donor of bpee shown, dotted lines indicate H-bonds).

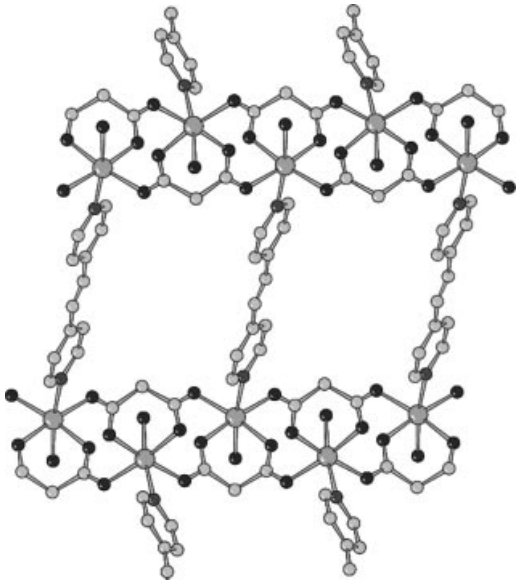

Figure 4. 3D crystal packing of complex **2** viewed down axis *a* showing layers connected by bpee ligands.

Table 2. Selected coordination bond lengths [Å] and angles [°] of complex **2**.

Mn–O(13)	2.165(3)	Mn–O(11)	2.183(3)
Mn–O(16)	2.172(3)	Mn–O(1w)	2.263(3)
Mn–O(17)	2.173(3)	Mn–N(21)	2.297(3)
O(13)–Mn–O(16)	99.24(12)	O(13)–Mn–N(21)	86.28(12)
O(13)–Mn–O(17)	90.15(12)	O(16)–Mn–N(21)	93.51(12)
O(16)–Mn–O(17)	170.60(11)	O(17)–Mn–N(21)	86.81(13)
O(13)–Mn–O(11)	173.19(12)	O(11)–Mn–N(21)	91.99(13)
O(16)–Mn–O(11)	87.43(12)	O(1w)–Mn–N(21)	172.13(13)
O(17)–Mn–O(11)	83.17(11)	C(12)–O(11)–Mn	127.9(2)
O(13)–Mn–O(1w)	88.59(11)	C(15)–O(17)–Mn	128.1(2)
O(16)–Mn–O(1w)	93.19(12)	C(12)–O(13′′)–Mn′′	132.6(3)
O(17)–Mn–O(1w)	87.25(12)	C(15)–O(16′)–Mn′	127.6(3)
O(11)–Mn–O(1w)	92.41(12)		

Symmetry operations: (′) ½ + *x*, ½ – *y*, ½ + *z*, (′′) ½ + *x*, ½ – *y*, ½ – *z*

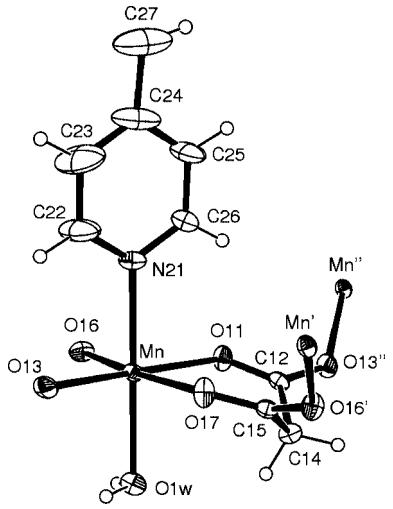

Figure 5. ORTEP drawing showing the coordination pattern of malonate anion in complex **2**.

The present structure is close comparable to those detected in analogous derivatives $[Mn_2(mal)_2(4,4\text{-bipy})(H_2O)_2]_n$,[6a] and $[Mn_2(mal)_2(hmt)(H_2O)_2]_n$,[6b] where $[Mn(mal)(H_2O)]_n$ layers are connected by 4,4′-bipy and hmt spacers, respectively. However, in the present complex **2**, the sheets are separated by 11.944 Å (half *b* axis), a longer value than that measured in closer packed layers of the 4,4′-bipy and hmt derivatives (9.386 and 8.029 Å, respectively). The intermetallic distance spaced by the bpee ligand is 14.052 Å, which is evidently longer than the value of 11.727 Å found in the 4,4′-bipy derivative.

A view of the packing along axis *a* evidences channels, accounting for 26.2% of the unit cell,[18] that are filled by disordered uncoordinated bpee and methanol molecules.

Complex 3

Complex **3**, of composition $[Mn_3(btc)_2(bipy)_2(H_2O)_6]\cdot 4(H_2O)$, forms a ladder-like ribbon built up of $Mn(H_2O)(bipy)$ and $Mn(H_2O)_4$ units bridged by btc anions as depicted in Figure 6. Of the two crystallographically independent manganese ions, Mn(1) possesses a distorted trigonal bipyramid coordination geometry (Figure 7). The equatorial plane encloses bipy nitrogen N(2) and btc oxygen donors O(2), O(4) [coordination distances of 2.289(8), 2.203(6), 2.204(6) Å, respectively], while bipy N(1) and aqua O(1w) are located at the axial sites [Mn(1)–N(1) = 2.242(9), Mn(1)–O(1w) = 2.132(7) Å]. However, oxygens O(1) and O(3) from different btc carboxylate groups at longer distance [Mn–O of 2.513(6), 2.528(6) Å] appear also to interact with the metal. This epta coordination pattern observed for Mn(1) is not novel, and, among other structures, it was reported in various Mn(EDTA) derivatives.[19] On the other hand, Mn(2) is located on a center of symmetry and attains the usual octahedral coordination geometry through four aqua ligands [Mn–OH_2 of 2.189(7),

2.206(8) Å] and two btc oxygens [Mn–O 2.156(6) Å]. A selection of coordination bond lengths and angles is reported in Table 3. Thus each btc ligand bridges three metal ions and the Mn_3 triangle have dimensions 10.096(4) Å along the Mn(1)–Mn(1) edge, 8.594(3) and 10.450(3) Å for the Mn(1)–Mn(2) edges. All the atoms of btc are coplanar within ± 0.14 Å, and the max deviation of metal ions from the best-fit-plane through the dianion is displayed by Mn(2) (Figure 6), being displaced by 0.34 Å. The distance measured between the btc centroids forming the (btc)-$Mn(H_2O)_4$-(btc) rungs of the stairlike chain is 11.59 Å.

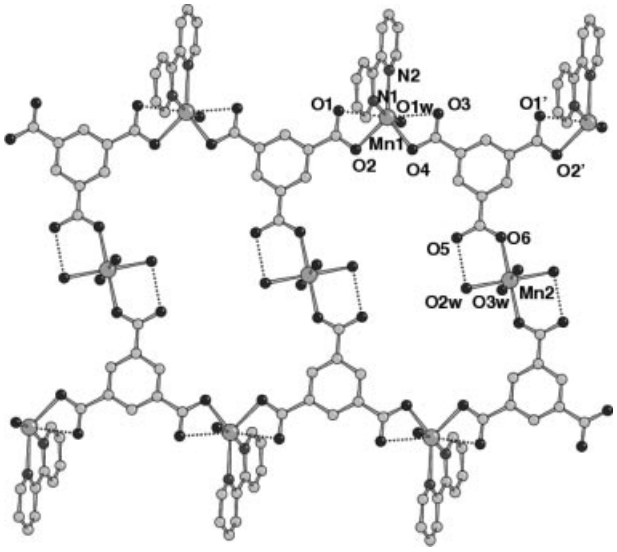

Figure 6. Double-stranded chain of complex **3** viewed down axis *c*. O(2w) forms an intrachain hydrogen bond, dotted lines Mn(1)–O(1) and Mn(1)–O(3) represent long coordination distances.

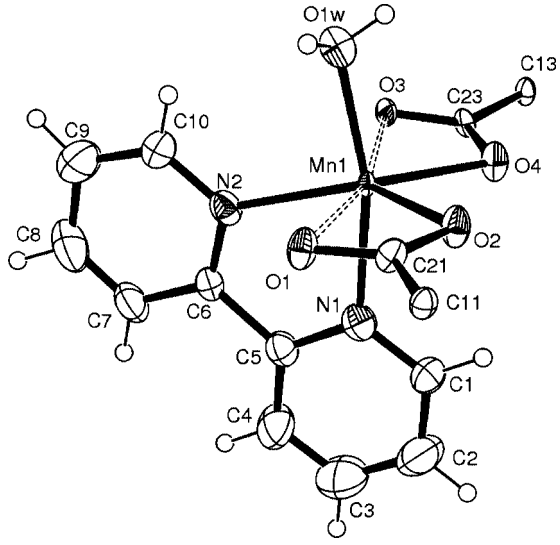

Figure 7. Detail of the coordination sphere of Mn(1) ion in complex **3** (ORTEP drawing, 40% probability level).

Table 3. Selected coordination bond lengths [Å] and angles [°] of complex **3**.

Mn(1)–N(1)	2.242(9)	Mn(1)–O(1)	2.528(6)
Mn(1)–N(2)	2.289(8)	Mn(1)–O(3)	2.513(6)
Mn(1)–O(1w)	2.132(7)	Mn(2)–O(2w)	2.189(7)
Mn(1)–O(2)	2.203(6)	Mn(2)–O(3w)	2.206(8)
Mn(1)–O(4)	2.204(6)	Mn(2)–O(6)	2.156(6)
N(1)–Mn(1)–N(2)	72.1(3)	O(2)–Mn(1)–O(3)	137.5(2)
O(1w)–Mn(1)–N(1)	165.6(3)	N(1)–Mn(1)–O(3)	96.6(2)
O(2)–Mn(1)–N(1)	93.0(3)	N(2)–Mn(1)–O(3)	84.3(2)
O(4)–Mn(1)–N(1)	92.1(3)	O(6)–Mn(2)–O(6′)	180.0
O(1w)–Mn(1)–N(2)	93.6(3)	O(3w)–Mn(2)–O(3w)	180.0
O(2)–Mn(1)–N(2)	137.7(2)	O(2w)–Mn(2)–O(2w′)	180.0
O(4)–Mn(1)–N(2)	135.2(3)	O(6)–Mn(2)–O(2w)	89.0(2)
O(1w)–Mn(1)–O(2)	96.9(3)	O(6′)–Mn(2)–O(2w)	91.0(2)
O(1w)–Mn(1)–O(4)	99.4(3)	O(6)–Mn(2)–O(3w)	88.4(3)
O(2)–Mn(1)–O(4)	83.1(2)	O(6′)–Mn(2)–O(3w)	91.6(3)
O(2)–Mn(1)–O(1)	55.3(2)	O(2w)–Mn(2)–O(3w)	87.4(3)
O(4)–Mn(1)–O(3)	55.3(2)	O(2w′)–Mn(2)–O(3w)	92.6(3)
O(3)–Mn(1)–O(1)	165.73(19)	C(21)–O(1)–Mn(1)	84.1(5)
O(1w)–Mn(1)–O(1)	89.4(2)	C(21)–O(2)–Mn(1)	98.9(5)
O(4)–Mn(1)–O(1)	138.3(2)	C(23)–O(3)–Mn(1)	84.3(4)
N(1)–Mn(1)–O(1)	87.8(3)	C(23)–O(4)–Mn(1)	98.5(5)
N(2)–Mn(1)–O(1)	84.1(2)	C(25)–O(6)–Mn(2)	130.8(5)
O(1w)–Mn(1)–O(3)	83.0(2)		

In the crystal packing the 1D chains are connected by a H-bonding Scheme that occurs among coordinated and lattice water molecules with carboxylate groups (Table 4). The shortest interchain Mn–Mn distance is 6.306(2) Å. The framework is locked through π-π interactions between the peripheral bipyridine ligands (Figure 8), enhancing the dimensionality of the complex to 3D. The $[Mn_3(btc)_2(bipy)_2(H_2O)_6]$ framework shows an accessible porosity that accounts for 20.4% of the unit cell volume (Platon program[18]): this space is occupied by lattice water molecules (four per metal unit). The present compound is isomorphous with that of cobalt derivative,[8k] where the uncoordinated water molecules were found disordered over different locations.

Table 4. Hydrogen bonding in complex **3**.

D–H	*d*(D–H)	*d*(H–A)	∠ D–H–A	*d*(D–A)	*A*[a]
O1w–H1	0.846	1.888	158.22	2.692(9)	O5 [–*x* + 1, –*y* + 2, –*z* + 1]
O1w–H2	0.838	1.994	154.91	2.776(12)	O4w [*x* + 1, *y*, *z*]
O2w–H1	0.851	2.048	145.75	2.793(9)	O5 [–*x* + 1, –*y* + 2, –*z* + 1]
O2w–H2	0.844	2.126	130.31	2.748(9)	O3 [–*x* + 1, –*y* + 1, –*z* + 1]
O3w–H1	0.849	1.977	147.18	2.730(10)	O1
O3w–H2	0.855	2.042	150.78	2.820(14)	O5w [–*x* + 1, –*y* + 1, –*z* + 2]

[a] The acceptor atoms O4w, O5w are lattice water molecules for which hydrogen atoms were not located.

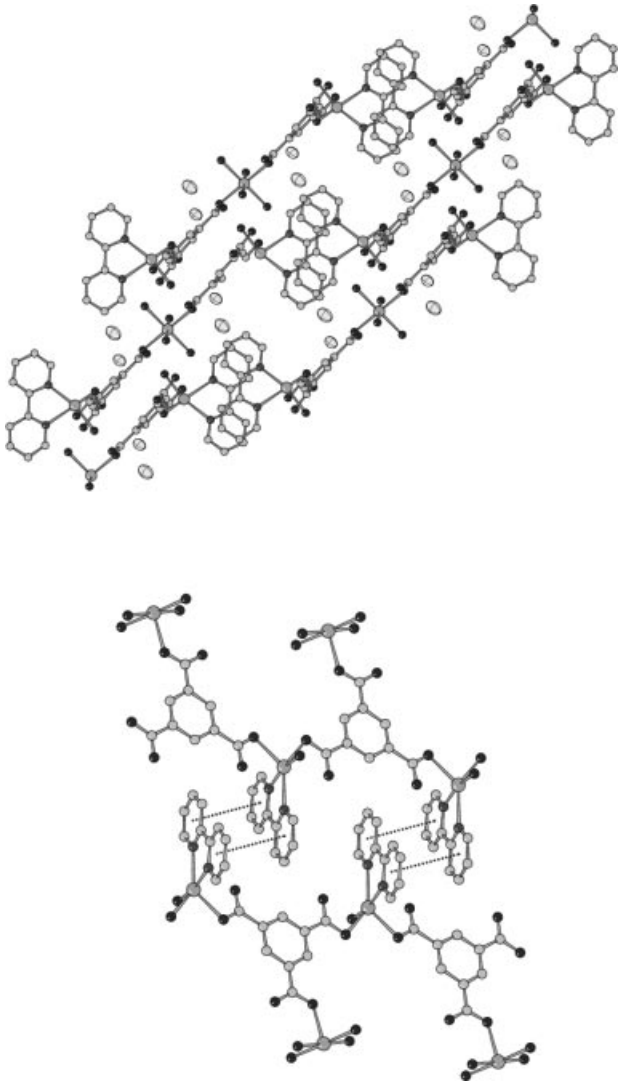

Figure 8. Top: packing diagram down axis *a* of complex **3** showing the π-π interactions between bipy ligands (ellipsoids represent lattice water oxygens). Bottom: detail of adjacent polymers with stacking bipy.

Magnetic Properties

Complex 1

Although the structure is two-dimensional, from a magnetic point of view the system can be considered as one-dimensional owing to the long Mn–Mn distance created by the linker dpyo, for which we can assume a negligible overlap between the magnetic orbitals of the Mn^{II} ions.

The temperature dependence of $\chi_M T$ (χ_M being the magnetic susceptibility for one Mn^{II} ion) for complex **1** is shown in Figure 9 (from 300 K to 2 K). At 300 K χ_M is 0.018 cm^3 mol^{-1}, and decreasing the temperature the χ_M value increases in a monotonous form up to 0.13 cm^3 mol^{-1} at 18 K, where the curve presents a maximum, and then decreases to 0.09 cm^3 mol^{-1} at 2 K. The value of $\chi_M T$ at 300 K is 4.6 cm^3 mol^{-1} K, which is as expected for an "isolated" Mn^{II} ion (Figure 9). Decreasing the temperature $\chi_M T$ gradually decreases reaching 0.2 cm^3 mol^{-1} K at 2.00 K. The shape of these curves is characteristic of the occurrence of antiferromagnetic interactions between the Mn^{II} centers and the presence of a maximum in the χ_M curve (Figure 9) indicates that the AF coupling is not negligible. The plot of the reduced magnetization ($M/N\beta$) at 2 K from 0 to 5 T is also indicative of the antiferromagnetic coupling (Figure 9, inset). The curve reaches the value of 1.2 $N\beta$, instead of 5.0 for an isolated $S = 2.5$ ion at 2 K, assuming $g = 2.00$. The X-band powder EPR spectrum at room temperature gives an isotropic signal centered at $g = 2.00$, typical for manganese(II) ions (Figure 1S).

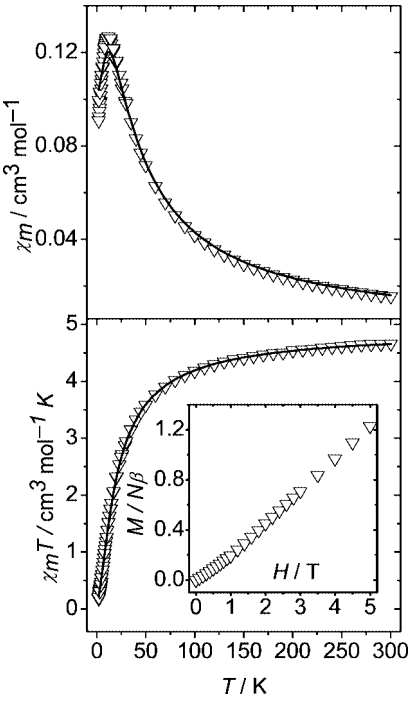

Figure 9. Plots of χ_M and $\chi_M T$ vs. T for complex **1**. Solid lines represent the best fit by using the expression cited in the text. Inset: plot of the reduced magnetization at 2 K.

This kind of magnetism for one-dimensional Mn^{II} system has been theoretically studied mainly by Fisher.[20] His approach allows to analyze the magnetic data by means of an analytical expression assuming an infinite number of classical spins ($S = 5/2$).[20] The best fit was obtained for $J = -1.89 \pm 0.01$ cm^{-1}, $g = 2.00 \pm 0.004$ and $R = 5.4 \times 10^{-5}$ (R is the agreement factor defined as $\Sigma_i[(\chi_M T)_{obs} - (\chi_M T)_{calc}]^2 / \Sigma_i[(\chi_M T)_{obs}]^2$). The value of $g = 2.00$ perfectly agrees with that expected for a manganese(II) ion ($S = 5/2$).

Scarce J data for manganese ions bridged by the oxalate ligand have been reported. In an excellent paper of Glerup et al.,[14] comparing the coupling in μ-oxalate complexes with manganese, iron, cobalt, and nickel, the mean value of J for three different Mn–oxalato complexes is –2.14 cm^{-1}, analogous to that found in complex **1**.

Complex 2

Before describing the features of complex **2**, we would like to recall that carboxylate functionality is among the most widely used bridging groups for designing polynuclear

complexes with interesting magnetic properties. Its versatility as a linker is illustrated by the variety of its coordination modes while acting as a bridge,[21] the most common being indicated as *syn-syn*, *syn-anti* and *anti-anti*. Usually the exchange coupling through the carboxylate moiety is highly dependent on the conformation of the bridge between the interacting metal centers.[22] The *syn-anti* bridge for carboxylate ligands appears to be a rather common binding mode for Mn^{II} complexes,[23] and a little is known about the magnetic properties of such complexes. In general, these bridges induce much smaller J values because of the expanded metallic core and the mismatch in the orientation of magnetic orbitals.[23] The magnetic properties for *syn-anti* Mn^{II}-carboxylato bridged complexes have been studied for some two-dimensional polymers such as $[Mn(MCPA)_2(H_2O)_2]_n$ (MCPA = 2-methyl-4-chlorophenoxyacetic acid),[24] for some one-dimensional polymers such as $[Mn(\mu\text{-}3\text{-}ClPhCOO)_2(2,2'\text{-bipy})_2]_n{\cdot}nH_2O$,[25] with two *syn-anti* carboxylate bridges and for discrete Mn^{II} homodinuclear complexes involving either only one *syn-anti* carboxylate bridge, $[Mn(2,2'\text{-bipy})_2(H_2O)_2(Me_2NCH_2COO)](ClO_4)$[26] or two *syn-anti* carboxylate bridges, $[Mn_2(\mu\text{-}PhCOO)_2(2,2'\text{-bipy})_4](ClO_4)_2$.[25] The antiferromagnetic coupling is always very small. In the presence of two carboxylate bridges[25] the coupling parameter J is slightly greater than that derived for a single bridge.[25,26] All these exchange coupling constants are of the same order (between –0.5 and –2 cm^{-1}).

The temperature dependence of $\chi_M T$ (χ_M being the magnetic susceptibility for one Mn^{II} ion) for complex **2** is shown in Figure 10 (top; from 300 K to 2 K). At 300 K χ_M is 0.0012 $cm^3\ mol^{-1}$ (Figure 2S) and it increases in a monotonous form to 0.65 $cm^3\ mol^{-1}$ at 2 K as the temperature is lowered. At 300 K $\chi_M T$ is 4.35 $cm^3\ mol^{-1}$ K, a value which is as expected for an "isolated" Mn^{II} ion. $\chi_M T$ is almost invariable up to 100 K and gradually decreases on cooling to reach the value of 1.3 $cm^3\ mol^{-1}$ K at 2.00 K. The shape of these curves is characteristic of the occurrence of weak antiferromagnetic interactions between the Mn^{II} centers. The lack of a maximum in the χ_M curve (Figure 2S) indicates that the AF coupling is very small. The plot or the reduced magnetization ($M/N\beta$) at 2 K from 0 to 5 T is also indicative of small antiferromagnetic coupling (Figure 10, bottom). The curve reaches the value of 4.7 $N\beta$, but the shape is different from the Brillouin function for an isolated $S = 2.5$ ion at 2 K, assuming $g = 2.00$.

Taking into account the structure of **2** in which Mn(mal) layers are linked together by the long bpee ligands, the susceptibility data were fitted by the expansion series of Lines[27] for a $S = 5/2$ antiferromagnetic quadratic layer, based on the exchange Hamiltonian $H = -\Sigma_{nn} J S_i S_j$, where Σ_{nn} runs over all pairs of nearest-neighbor spins i and j, Equation (1).

$$Ng^2\beta^2/\chi|J| = 3\theta + (\Sigma C_n/\theta^{n-1}) \quad (1)$$

$\theta = kT/|J|S(S+1)$, $C_1 = 4$, $C_2 = 1.448$, $C_3 = 0.228$, $C_4 = 0.262$, $C_5 = 0.119$, $C_6 = 0.017$ and N, g and β in Equation (1) have their usual meanings. The best fit is obtained for the superexchange parameters $J = -0.20 \pm 0.02$ cm^{-1} and $g = 2.00 \pm 0.003$ (Figure 10) with $R = 2.6 \times 10^{-4}$.

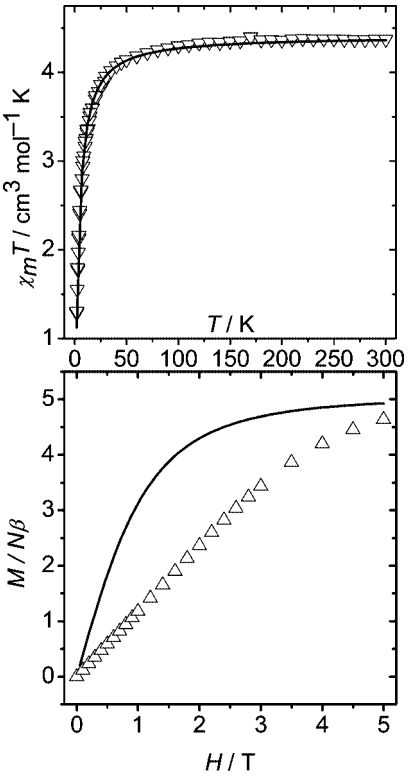

Figure 10. Top: plot of the $\chi_M T$ vs. T for complex **2**. Solid line represents the fit with the expression given in the text. Bottom: plot of the reduced magnetization at 2 K. Solid line represents the Brillouin function for $S = 2.5$ and $g = 2.00$.

The magnetic properties of **2** may be compared with those observed of other two-dimensional manganese(II) systems showing low antiferromagnetic coupling and for which possible antiferromagnetic ordering is not yet achieved at the lowest limit of the measurement temperature. For example, in $[\{Mn(SCN)_2(EtOH)_2\}_2]$,[27b] the superexchange parameter J was reported to be –1.22 cm^{-1} and the low-temperature EPR spectra show an increase in the line width at low temperature, but the susceptibility plot does not show important deviations from the theoretical two-dimensional susceptibility plot even not at low temperature. Room temperature X-band EPR spectrum (Figure 3S) shows an isotropic signal centered at $g = 2.00$, typical for manganese(II) ions.

Complex 3

Plot of $\chi_M T$ vs. T for complex **3** is shown in Figure 11 (top). At 300 K $\chi_M T$ starts at 4.36 $cm^3\ mol^{-1}$ K, which is the typical value for one isolated Mn^{II} ion ($g = 2.00$). This value is almost constant up to 50 K, then it decreases rapidly to 3.62 $cm^3\ mol^{-1}$ K at 2 K, a trend indicative of very weak antiferromagnetic coupling among the manganese(II) ions. The reduced magnetization curve ($M/N\beta$) vs. H at 2 K corroborates this very weak antiferromagnetic coupling. The experimental data are slightly smaller than those corresponding to the Brillouin function for $S = 5/2$

and g = 2.00 (Figure 11, bottom). This almost negligible antiferromagnetic coupling is due to the extended benzenetricarboxyalate bridging ligand, which cannot create any significant coupling.[28]

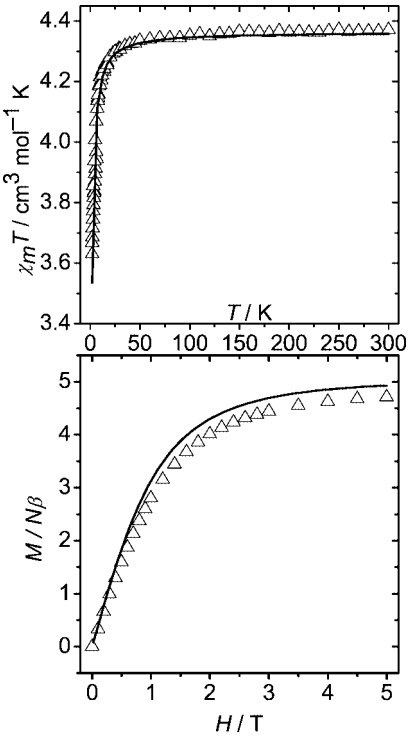

Figure 11. Top: plot of $\chi_M T$ vs. T for complex **3** with the best fit calculation represented by the solid line. Bottom: plot of the reduced magnetization vs. H at 2 K. Solid line corresponds to the Brillouin function for g = 2.00.

The magnetic fit for complex **3** is impracticable, due to its intrinsic complication. Considering the structure as a pseudo-one-dimensional Mn^{II} systems (S = 5/2) it is possible to try to fit the experimental susceptibility data by using the formula given by Fisher for a model with classical spin.[20,22] The best fit parameters were J = –0.05 cm^{-1}, g = 2.00 and $R = 1.8 \times 10^{-3}$. However, J value must be taken cautiously, being the one-dimensionality only a drastic estimate, and thus the Fisher's formula would not be completely valid. Furthermore, the asymmetry of one of the manganese ions could give a g value different from 2.00, likely indicative that the hypothesis of the g = 2.00 in the reduced magnetization is not fully accurate, and the AF coupling is even lower than –0.05 cm^{-1}. The X-band powder EPR spectrum at room temperature shows an isotropic signal centered at g = 2.00. (Figure 4S).

Thermal Analysis

Complex **1** upon heating does not show any mass change up to 300 °C and on further heating its frame work gradually collapses. The thermogravimetric analysis of complex **2** shows desolvation within the temperature range of 70–200 °C (Figure 5S). The behavior suggests the loss of lattice methanol and dehydration of coordinated water molecules (vide infra) takes place in sequence without showing any intermediate species. This also corroborates the involvement of H-bonding between the malonate oxygens and water molecules. The lattice bpee cannot leave the system upon heating up to 200 °C, then the framework of the complex collapses. On the other hand complex **3**, that comprises of ten water molecules per trinuclear unit, loses water in multi steps upon heating (Figure 6S). The first step (60–125 °C) accounts for the release of four guest water as well as two coordinated water molecules. This upon further heating starts to lose coordinated water molecules showing a non isolable intermediate at ca. 200 °C and then the framework appears to collapse on continuation of heating. Through careful heating we have been able to isolate the intermediate, $[Mn_3(btc)_2(2,2'\text{-bipy})_2(H_2O)_4]$ (**3a**) which reverts on exposure to humid atmosphere (≈ 70%) for 2–3 hours. The formation of **3a** is not unlikely as elimination of one water molecule from each terminal metal center results in a six coordinated geometry for Mn(1) (see Figure 7), but further elimination of coordinated water molecules leads to an unstable system and to the collapse of the metal organic framework. Thus the thermal analyses of these three complexes hint that the MOF of **1** is thermally more stable than those of **2** and **3**.

Conclusions

In this paper we have presented the syntheses, the crystal structures, variable temperature magnetic studies and thermal behaviors of three carboxylato-bridged polymeric networks of manganese(II). The above discussion shows that the use of different carboxylates, namely oxalate, malonate and 1,3,5-benzenetricarboxylate, in combination with neutral coligands, dpyo, bpee, and 2,2′-bipy, has made feasible the construction of coordination polymers of different dimensionality. Complexes **2** and **3** are 3D open frameworks, the former contains channels filled up by disordered uncoordinated bpee and methanol and the latter is achieved through π-π and H-bonding interactions. On the other hand, complex **1** is a covalent bonded 2D network.

Experimental Section

Materials: High purity manganese chloride tetrahydrate; 4,4′-bipyridyl *N*,*N*′-dioxide; 2,2′-bipyridine and *trans*-1,2-bis(4-pyridyl)ethylene were purchased from Aldrich chemical Company. All other chemicals used were of analytical grade.

Physical Measurements: Elemental analyses (carbon, hydrogen and nitrogen) were performed using a Perkin–Elmer elemental analyzer. IR spectra (4000–600 cm^{-1}) were taken in KBr pellets using a Jasco FT-IR (model 300E). The magnetic measurements were carried out on polycrystalline samples with a Quantum Design MPMS SQUID magnetometer (applied field 0.1 T) working in the temperature range 300–2 K. Diamagnetic corrections were estimated from Pascal's tables. EPR spectra were recorded on powder samples at X-band frequency with a BRUKER 300E automatic spectrometer, varying the temperature between 4–300 K. Thermal analysis were done on a Pyris Diamond system.

Table 5. Crystal data and refinements details of complexes **1**, **2** and **3**.

	1	**2**	**3**
Formula	$C_{12}H_8MnN_2O_6$	$C_{24.50}H_{25}Mn_2N_3O_{10.50}$	$C_{38}H_{42}Mn_3N_4O_{22}$
M_r [g mol^{-1}]	331.14	639.35	1071.58
Crystal system	monoclinic	monoclinic	triclinic
Space group	$C2/c$	$P2_1/n$	$P\bar{1}$
a [Å]	14.231(3)	7.413(4)	10.096(4)
b [Å]	5.657(2)	23.889(5)	10.756(4)
c [Å]	15.189(3)	7.467(4)	12.167(5)
α [°]			74.097(10)
β [°]	94.59(2)	92.224(10)	76.083(10)
γ [°]			81.210(10)
Volume [Å^3]	1218.9(6)	1321.3(10)	1228.0(8)
Z	4	2	1
$D_{calcd.}$ [g cm^{-3}]	1.805	1.607	1.449
μ, Mo-K_α [mm^{-1}]	1.115	1.020	0.840
θ_{max} [°]	26.41	25.73	26.21
Reflections collected	5256	7634	6091
Unique reflections	1187	2338	3560
R_{int}	0.0710	0.0314	0.0418
Refined parameters	96	223	323
Goodness of fit (F^2)	0.923	1.129	1.082
R_1 [$I > 2\sigma(I)$][a]	0.0365	0.0529	0.0983
wR_2[a]	0.0823	0.1225	0.2602

[a] $R_1(F_o) = \Sigma \, ||F_o| - |F_c||/\Sigma|F_o|$, $wR_2(F_o^2) = [\Sigma w(F_o^2 - F_c^2)^2/\Sigma w(F_o^2)^2]^{1/2}$.

Crystallographic Data Collection and Refinement: Crystal data and details of data collections and refinements for the structures reported are summarized in Table 5. Diffraction data set of complex **1** was carried out on a Nonius DIP-1030H system with Mo-K_α radiation. For complexes **2** and **3**, reflections were collected on a STOE four–circle diffractometer equipped with MAR–research image plate system and Mo-K_α radiation. Cell refinement, indexing and scaling of the data sets were carried out using Denzo and Scalepack,[29] and XDS.[30] All the structures were solved by Patterson and Fourier analyses[31] and refined by the full-matrix least-squares method based on F^2 with all observed reflections.[31] Two lattice water molecules were detected in the ΔF map of complex **3**. Disordered peaks in the electron-density map of complex **2** were interpreted as a bpee ligand and a methanol (both arranged over a center of symmetry), each accounting for 0.25 molecule per metal unit. The contribution of H atoms at calculated positions were included in the final cycles of refinement, except those of lattice water and disordered molecules. All the calculations were performed using the WinGX System 1.64.05.[32]

[Mn(ox)(dpyo)]$_n$ (1): A methanolic solution (10 mL) of 4,4′-bipyridine *N*,*N*′-dioxide (1 mmol, 0.188 g) was added dropwise to an aqueous solution (5 mL) of $MnCl_2{\cdot}4H_2O$ (1 mmol, 0.197 g) with constant stirring for 10 min. To the resulting reaction mixture an aqueous solution of disodium oxalate (1 mmol, 0.134 g) was added whilst stirring condition. After 30 minutes a bright red compound separated. Single crystals suitable for X-ray analysis were obtained by diffusing a methanolic solution (10 mL) of $MnCl_2{\cdot}4H_2O$ and 4,4′-bipyridine *N*,*N*′-dioxide on an aqueous solution (10 mL) of disodium oxalate in a tube. Bright red crystals deposited at the junction of two solutions after one week. Yield: 80%. $C_{12}H_8MnN_2O_6$ (331.14): C 43.48, H 2.41, N 8.45; found C 43.47, H 2.42, N 8.46. IR: $\tilde{\nu}$ = 3114 (w), 3085 (w), 2929 (vw), 1619 (vs), 1468 (s), 1222 (s), 1176 (w), 844 (w), 792 (vw), 553 (vw) cm^{-1}.

{[Mn$_2$(mal)$_2$(bpee)(H$_2$O)$_2$]·0.5(bpee)·0.5(CH$_3$OH)}$_n$ (2): An aqueous solution (5 mL) of disodium malonate (1 mmol, 0.148 g) was added to an aqueous solution (5 mL) of $MnCl_2{\cdot}4H_2O$ (1 mmol, 0.197 g) whilst stirring condition. To this reaction mixture a methanolic solution (10 mL) of *trans*-1,2-bis(4-pyridyl)ethylene (1 mmol, 0.182 g) was added. The resultant reaction mixture was stirred for 1 h and filtered. The filtrate was kept in a desiccator ($CaCl_2$) and after a few days bright yellow single crystals of X-ray diffraction quality were obtained. Yield 75%. $C_{24.50}H_{25}Mn_2N_3O_{10.50}$ (639.35): C 45.98, H 3.91, N 6.56; found C 46.01, H 3.90, N 6.57. IR: $\tilde{\nu}$ = 3436-3190 (s, v br), 1675 (w), 1611 (vs), 1558 (vs), 1467 (w), 1436 (s), 1372 (vs), 1314 (w), 1104 (w), 1016 (w), 830 (w), 761 (s), 731 (s), 628 (w), 542 (w) cm^{-1}.

{[Mn$_3$(btc)$_2$(2,2′-bipy)$_2$(H$_2$O)$_6$]·4H$_2$O}$_n$ (3): An aqueous solution (5 mL) of $MnCl_2{\cdot}4H_2O$ (1 mmol, 0.197 g) was added to a methanolic solution of (10 mL) of 2,2′-bipyridine (1 mmol, 0.156 g) dropwise whilst stirring condition. The resultant yellow colored solution was mixed to an aqueous solution (5 mL) of btc (0.66 mmol, 0.184 g) and stirred for 1 h and filtered. The filtrate was kept in a desiccator ($CaCl_2$). After one week bright yellow crystals suitable for X-ray diffraction were obtained. Yield 70%. $C_{38}H_{42}Mn_3N_4O_{22}$ (1071.58): C 42.55, H 3.91, N 5.22, found C 42.57, H 3.93, N 5.20. IR: $\tilde{\nu}$ = 3475–3025 (s, v br) 1671 (w), 1611 (vs), 1557 (vs), 1437 (s), 1372 (s), 1314 (w), 1247 (w), 1157 (w), 1016 (w), 932 (w), 761 (s), 731 (s), 650 (w), 541 (w) cm^{-1}.

CCDC-276231, -276232 and -276233 (for complexes **1**, **2** and **3**, respectively) contain the supplementary crystallographic data for this paper. These data can be obtained free of charge from The Cambridge Crystallographic Data Centre via www.ccdc.cam.ac.uk/data_request/cif.

Supporting Information (for details see the footnote on the first page of this article): X-band EPR spectra for complexes **1**–**3**, the χ_M plot vs. T for **2**, and the thermogravimetric analysis of **2** and **3** (Figures 1S–6S).

Acknowledgments

N. R. C. thanks Council of Scientific and Industrial Research, New Delhi, and J.R. thanks Spanish Government for financial support (BQU2003/00539).

[1] a) H. K. Chae, D. Y. Siberio-Perez, J. Kim, Y. B. Go, M. Eddaoudi, A. J. Matzger, M. O'Keeffe, O. M. Yaghi, *Nature* **2004**, *427*, 523; b) A. I. Skoulidas, *J. Am. Chem. Soc.* **2004**, *126*, 1356; c) N. L. Rosi, J. Eckert, M. Eddaoudi, D. T. Vodak, J. Kim, M. O'Keeffe, O. M. Yaghi, *Science* **2003**, *300*, 1127; d) M.-L. Tong, S. Kitagawa, H.-C. Chang, M. Ohba, *Chem. Commun.* **2004**, 418; e) S. C. Zimmerman, M. S. Wendland, N. A. Rakow, I. Zharov, K. S. Suslick, *Nature* **2002**, *418*, 399; f) A. Katz, M. E. Davis, *Nature* **2000**, *403*, 286; g) X.-J. Zheng, L.-C. Li, S. Gao, L.-P. Jin, *Polyhedron* **2004**, *23*, 1257; h) M. Tominaga, S. Tashiro, M. Aoyagi, M. Fujita, *Chem. Commun.* **2002**, 2038; i) K. Biradha, M. Fujita, *Angew. Chem. Int. Ed.* **2002**, *41*, 3392; j) O. R. Evans, W. Lin, *Acc. Chem. Res.* **2002**, *35*, 511.

[2] a) D. W. Bruce, D. O'Hare. *Inorganic Materials*, Eds. John Wiley & Sons New York **1992**; b) R. D. Willet, D. Gatteschi, O. Kahn. *Magneto Structural Correlations in Exchange Coupled System* Eds. NATO ATI Series C140; Reidal: Dordrecht, The Netherlands **1985**; c) B. Multon, M. J. Zaworotko, *Chem. Rev.* **2001**, *101*, 1629; d) P. J. Hagrman, D. Hagrman, J. Zubieta, *Angew. Chem. Int. Ed.* **1999**, *38*, 2638; e) R. Robson, *J. Chem. Soc., Dalton Trans.* **2000**, 3735; f) W. Su, M. Hong, J. Weng, R. Cao, S. Lu, *Angew. Chem. Int. Ed.* **2000**, *39*, 2911; g) D. Gatteschi, O. Kahn, J. Miller, *Molecular Magnetic Materials* Eds. Nato ASI Series EI98; Kluwer. Dordrecht, The Netherlands, **1991**; h) O. M. Yaghi, G. Li, H. Li, *Nature* **1995**, *378*, 703; i) K. Marouka, N. Murase, H. Yamamoto, *J. Org. Chem.* **1993**, *58*, 2938; j) C. Chen, K. S. Suslick, *Coord. Chem. Rev.* **1993**, *128*, 293 and references cited therein; k) O. C. Montelro, H. I. S. Noguelra, T. Trindade, *Chem. Mater.* **2001**, *13*, 2103; l) A. J. Waddon, E. B. Coughlin, *Chem. Mater.* **2003**, *15*, 4555; m) M. Kondo, Y. Irie, Y. Shimizu, M. Miyazawa, H. Kawaguchi, A. Nakamura, T. Naito, K. Maeda, H. Uchida, *Inorg. Chem.* **2004**, *43*, 6139; n) S. C. Johannessen, R. G. Brisbois, *J. Am. Chem. Soc.* **2001**, *123*, 3818; o) J.-W. Park, E. L. Thomas, *J. Am. Chem. Soc.* **2002**, *124*, 515.

[3] a) Y. Cui, O. R. Evans, H. L. Ngo, P. S. White, W. Lin, *Angew. Chem. Int. Ed.* **2002**, *41*, 1159; b) D. K. Chand, K. Biradha, M. Fujita, S. Sakamoto, K. Yamaguchi, *Chem. Commun.* **2002**, 2486; c) L. Pan, X. Y. Huang, J. Li, Y. Wu, N. Zheng, *Angew. Chem. Int. Ed.* **2000**, *39*, 527; d) S. Takamizawa, E.-I. Nakata, H. Yokoyama, K. Mochizuki, W. Mori, *Angew. Chem. Int. Ed.* **2003**, *42*, 4331; e) J. Y. Lu, A. M. Babb, *Chem. Commun.* **2002**, 1340.

[4] a) L. Dubois, D.-F. Xiang, X.-S. Tan, J. Pécaut, P. Jones, S. Baudron, L. L. Pape, J.-M. Latour, C. Baffert, S. Chardon-Noblat, M.-N. Collomb, A. Deronzier, *Inorg. Chem.* **2003**, *42*, 750; b) C. N. R. Rao, S. Natarajan, R. Vaidhyanathan, *Angew. Chem. Int. Ed.* **2004**, *43*, 1466.

[5] a) S. Konar, P. S. Mukherjee, E. Zangrando, F. Lloret, N. Ray Chaudhuri, *Angew. Chem. Int. Ed.* **2002**, *41*, 1561; b) P. S. Mukherjee, T. K. Maji, G. Mostafa, J. Ribas, M. S. E. Fallah, N. Ray Chaudhuri, *Inorg. Chem.* **2001**, *40*, 928; c) S. Konar, E. Zangrando, N. Ray Chaudhuri, *Inorg. Chim. Acta* **2003**, *355*, 264.

[6] a) T. K. Maji, S. Sain, G. Mostafa, T.-H. Lu, J. Ribas, M. Monfort, N. Ray Chaudhuri, *Inorg. Chem.* **2003**, *42*, 709; b) S. Konar, S. C. Manna, E. Zangrando, T. Mallah, J. Ribas, N. Ray Chaudhuri, *Eur. J. Inorg. Chem.* **2004**, 4202; c) S. Sain, T. K. Maji, G. Mostafa, T.-H. Lu, N. Ray Chaudhuri, *Inorg. Chim. Acta* **2003**, *351*, 12.

[7] a) S. Sain, T. K. Maji, G. Mostafa, T.-H. Lu, N. Ray Chaudhuri, *New J. Chem.* **2003**, *27*, 185; b) S. Dalai, P. S. Mukherjee, E. Zangrando, F. Lloret, N. Ray Chaudhuri, *J. Chem. Soc., Dalton Trans.* **2002**, 822; c) S. Konar, P. S. Mukherjee, M. G. B. Drew, J. Ribas, N. Ray Chaudhuri, *Inorg. Chem.* **2003**, *42*, 2545; d) P. S. Mukherjee, S. Konar, E. Zangrando, T. Mallah, J. Ribas, N. Ray Chaudhuri, *Inorg. Chem.* **2003**, *42*, 2695; e) S. Konar, E. Zangrando, M. G. B. Drew, J. Ribas, N. Ray Chaudhuri, *Dalton Trans.* **2004**, 260.

[8] a) E. G. Bakalbassis, M. Korabik, A. Michailides, J. Mrozinski, C. Raptopoulou, S. Skoulika, A. Terzis, D. Tsaousis, *J. Chem. Soc., Dalton Trans.* **2001**, 850; b) C. Livage, C. Egger, M. Nogues, G. Férey, *J. Mater. Chem.* **1998**, *8*, 2743; c) C. Livage, C. Egger, G. Férey, *Chem. Mater.* **1999**, *11*, 1546; d) L.-S. Long, X.-M. Chen, M.-L. Tong, Z.-G. Sun, Y.-P. Ren, R.-B. Huang, L.-S. Zheng, *J. Chem. Soc., Dalton Trans.* **2001**, 2888; e) M.-X. Li, G.-Y. Xie, S.-L. Jin, Y.-D. Gu, M.-Q. Li, J. Liu, Z. Xu, X.-Z. You, *Polyhedron* **1996**, *15*, 535; f) J. J. Girerd, M. Verdaguer, *Inorg. Chem.* **1980**, *19*, 274; g) M. Julve, M. Verdaguer, A. Gleizes, M. Philoche-Lavisalles, O. Kahn, *Inorg. Chem.* **1984**, *23*, 3808; h) M. Julve, J. Faus, M. Verdaguer, A. Gleizes, *J. Am. Chem. Soc.* **1984**, *106*, 3808; i) L. Deakin, A. M. Ariff, J. S. Miller, *Inorg. Chem.* **1999**, *38*, 5072; j) M.-F. S. Lo, S.-Y. S. Chui, I. D. Willams, L. Y. Shek, Z. Lin, X. X. Zang, G. H. Wen, *J. Am. Chem. Soc.* **2000**, *122*, 6293; k) M. J. Plater, M. R. St. J. Foreman, E. Coronado, C. J. Gómez-García, A. M. Z. Slawin, *J. Chem. Soc., Dalton Trans.* **1999**, 4209.

[9] a) *Magneto Structural Correlations in Exchange Coupled Systems* (Eds.: R. D. Willet, D. Gatteschi, O. Kahn); NATO ASI Series C140; Reidel: Dordrecht, The Netherlands, **1985**.

[10] a) C. Janiak, *Dalton Trans.* **2003**, 2781; b) C.-T. Chen, K. S. Suslick, *Coord. Chem. Rev.* **1993**, *128*, 293; c) O. Kahn, J. Larionova, L. Ouahab, *Chem. Commun.* **1999**, 945; d) J. Cernak, M. Orendac, I. Potocnak, J. Chomic, A. Orendacova, J. Skorsepa, A. Feher, *Coord. Chem. Rev.* **2002**, *224*, 51; e) O. Sato, I. Iyoda, A. Fujishima, K. Hashimoto, *Science* **1996**, *271*, 49; f) T. Mallah, S. Thiebaut, M. Verdaguer, P. Veillet, *Science* **1993**, *262*, 1554.

[11] G. Christou, D. Gatteschi, D. N. Hendrickson, R. Sessoli, *MRS Bull.* **2000**, *25*, 66.

[12] G. Aromí, S. M. J. Aubin, M. A. Bolcar, G. Christou, H. J. Eppley, K. Folting, D. N. Hendrickson, J. C. Huffman, R. C. Squire, H.-L. Tsai, S. Wang, M. W. Wemple, *Polyhedron* **1998**, *17*, 3005.

[13] a) R. Sessoli, D. Gatteschi, A. Caneschi, M. A. Novak, *Nature* **1993**, *365*, 141; b) G. Christou, in: *Magnetism: A Supramolecular Function* (Ed.: O. Kahn); NATO Series; Kluwer: Dordrecht, The Netherlands, **1996**; pp. 383–410; c) R. Sessoli, H.-L. Tsai, A. R. Schake, S. Wang, J. B. Vincent, K. Folting, D. Gatteschi, G. Christou, D. N. Hendrickson, *J. Am. Chem. Soc.* **1993**, *115*, 1804.

[14] J. Glerup, P. A. Goodson, D. J. Hodgson, K. Michelsen, *Inorg. Chem.* **1995**, *34*, 6255.

[15] a) E. Coronado, J. R. Galán-Mascarós, C. J. Gómez-García, J. M. Martínez-Agudo, *Inorg. Chem.* **2001**, *40*, 113; b) E. Coronado, J. R. Galán-Mascarós, C. J. Gómez-García, E. Martínez-Ferrero, S. V. Smaalen, *Inorg. Chem.* **2004**, *43*, 4808; c) A. Alberola, E. Coronado, J. R. Galán-Mascarós, C. Giménez-Saiz, C. J. Gómez-García, *J. Am. Chem. Soc.* **2003**, *125*, 10774.

[16] P. Lightfoot, A. Snedden, *J. Chem. Soc., Dalton Trans.* **1999**, 3549.

[17] T. Lis, J. Matuszewski, *Acta Crystallogr., Sect. B* **1979**, *35*, 2212.

[18] A. L. Spek, *Acta Crystallogr., Sect. A* **1990**, *46*, C34.

[19] a) S. Richards, B. Pedersen, J. V. Silverton, J. L. Hoard, *Inorg. Chem.* **1964**, *3*, 27; b) X. Solans, S. Gali, M. Font-Altaba, J. Oliva, J. Herrera, *Afinidad* **1988**, *45*, 243.

[20] M. E. Fisher, *Am. J. Phys.* **1964**, *32*, 343.

[21] C. Oldham, in: *Comprehensive Coordination Chemistry*; (Eds.: G. Wilkinson, R. D. Gillard, J. A. McCleverty); Pergamon Press: Oxford, **1987**; Vol. 2, p. 435.

[22] O. Kahn, *Molecular Magnetism*, VCH, New York, **1993**.

[23] C. Policar, F. Lambert, M. Cesario, I. Morgenstern-Badarau, *Eur. J. Inorg. Chem.* **1999**, 2201 and references cited therein.

[24] V. Tangoulis, G. Psomas, C. Dendrinou-Samara, C. P. Raptopoulou, A. Terzis, D. P. Kessissoglou, *Inorg. Chem.* **1996**, *35*, 7655.

[25] B. Albela, M. Corbella, J. Ribas, I. Castro, J. Sletten, H. Stoeckli-Evans, *Inorg. Chem.* **1998**, *37*, 788.

[26] X. M. Xen, Y. X. Tong, Z. T. Xu, T. C. W. Mak, *J. Chem. Soc., Dalton Trans.* **1995**, 4001.
[27] a) M. E. Lines, *J. Phys. Chem. Solids* **1970**, *31*, 101; b) A. Escuer, R. Vicente, M. A. S. Goher, F. A. Mautner, *J. Chem. Soc., Dalton Trans.* **1997**, 4431 and references cited therein.
[28] H. J. Choi, M. P. Suh, *J. Am. Chem. Soc.* **1998**, *120*, 10622.
[29] Z. Otwinowski, W. Minor, "Processing of X-ray Diffraction Data Collected, in: Oscillation Mode", Methods in Enzymology, Volume 276: Macromolecular Crystallography (Eds.: C. W. Carter, Jr., R. M. Sweet) **1997**, part A, p. 307–326, Academic Press.
[30] W. Kabsch, *J. Appl. Cryst.* **1988**, *21*, 916.
[31] SHELX 97 Programs for Crystal Structure Analysis (Release 97–2). G. M. Sheldrick, University of Göttingen, Germany, **1998**.
[32] L. J. Farrugia, *J. Appl. Crystallogr.* **1999**, *32*, 837.

Received: June 27, 2005
Published Online: November 7, 2005

